Short-Term Peak-Shaving Operation of Head-Sensitive Cascaded Hydropower Plants Based on Spillage Adjustment

Shengli Liao [1], Yan Zhang [1], Benxi Liu [1,*] , Zhanwei Liu [1], Zhou Fang [1] and Shushan Li [2]

[1] Institute of Hydropower and Hydroinformatics, Dalian University of Technology, Dalian 116024, China; shengliliao@dlut.edu.cn (S.L.); zy-zhangyan@foxmail.com (Y.Z.); zhanweiliu@mail.dlut.edu.cn (Z.L.); fangzhou1225fz@mail.dlut.edu.cn (Z.F.)

[2] Power Dispatching Control Center of China Southern Power Grid, Guangzhou 510623, China; liss@csg.cn

* Correspondence: benxiliu@dlut.edu.cn

Abstract: There are many cascaded hydropower plants with poor regulation performance and sensitive water heads accompanied by water spillage during the wet season. Faced with the increasing load peak–valley differences, it is necessary to tap the peak-shaving potential of such head-sensitive cascaded hydropower plants (HSCHPs) because relying solely on hydropower plants with better regulation performance for peak shaving is inadequate. To address the modeling, solving, and water spillage treatment difficulties posed by HSCHPs, a new short-term peak-shaving method based on spillage adjustment is introduced. First, fuzzy cluster analysis is used to determine when to release more water spillage by automatically identifying valley periods of the daily load curve. Furthermore, a spillage adjustment strategy, implemented through an easy gate operation, is adopted to readjust the water release during each period of the load curve. The ratio of the water spillage released in advance in a certain period to its total water spillage is defined as the water spillage ratio (WSR) of the period. Finally, a mixed-integer linear programming model linearized by special ordered sets of type two is solved to determine the optimal WSRs, which achieves the optimal peak-shaving effect. HSCHPs in the Hongshui River Basin during the wet season were selected as case studies. The results demonstrate that the proposed method can achieve a good peak-shaving effect without significantly reducing the power generation and adding additional water spillage.

Keywords: head-sensitive cascaded hydropower plants; fuzzy clustering analysis; water spillage ratio; mixed-integer linear programming

1. Introduction

As the country with the richest hydropower potential in the world, China has made tremendous achievements in hydropower industry development during the past two decades [1]. By the end of 2019, China's installed hydropower generation capacity reached 356.4 GW [2] (18% of its total installed generation capacity), ranking first in the world. Affected by rainfall, the distribution of hydropower resources in China is uneven. A majority of hydropower bases are located in the southwest regions [3], especially in Yunnan, Sichuan, and Guangxi provinces. To effectively utilize the water head drop to generate electricity, most of these river basins have adopted cascaded structures, such as the eight-level structure of the middle stream of the Jinsha River and the ten-level structure of the Hongshui River. However, most of the downstream plants in cascaded hydropower systems are often low-head hydropower plants with poor regulation performance (take the Hongshui River cascade structure shown in Figure 1 as an example, where Pingban, Dahua, Bailongtan, Letan, and Qiaogong are such hydropower plants).
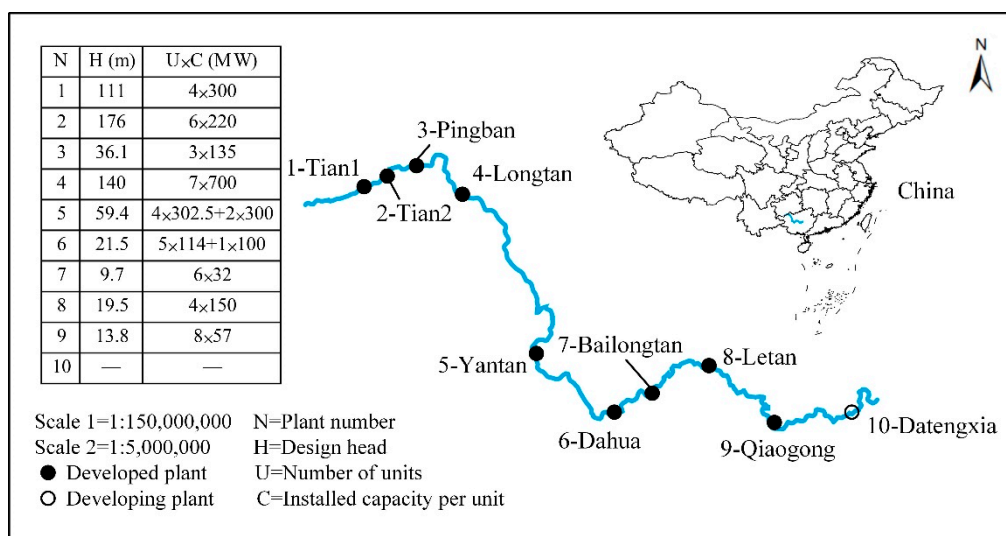
N	H (m)	U×C (MW)
1	111	4×300
2	176	6×220
3	36.1	3×135
4	140	7×700
5	59.4	4×302.5+2×300
6	21.5	5×114+1×100
7	9.7	6×32
8	19.5	4×150
9	13.8	8×57
10	—	—

Scale 1=1:150,000,000   N=Plant number
Scale 2=1:5,000,000   H=Design head
● Developed plant   U=Number of units
○ Developing plant   C=Installed capacity per unit

Figure 1. The Hongshui River cascade structure: Scale 1 is the scale of the map; Scale 2 is the scale of the river.

Although the construction of cascaded hydropower plants has greatly improved power generation efficiency, the forebay water level of the downstream plant is greatly affected by the water release of the upstream plant, resulting in large variations in the water head during a single day. Moreover, the power outputs of these plants are very sensitive to water heads [4]. For head-sensitive cascaded hydropower plants (HSCHPs), inaccurate consideration of water heads will lead to deviations between the planned and actual power outputs, which pose a threat to the safety operation of the power system. In addition, limited by poor regulation performance, water spillage is inevitable when HSCHPs participate in short-term scheduling during the wet season. In 2018, the loss of electric quantity due to water spillage was approximately 69.1 billion kWh [5], almost one fifth of the total power generation in the UK in 2018 [6]. Due to the construction of many cascaded hydropower plants with poor regulation performance, China's Sichuan and Yunnan provinces generate lots of water spillage during the wet season. From 2013 to 2018, the loss of electric quantity due to water spillage in Sichuan increased from 2.6 billion to 12.2 billion kWh, and that in Yunnan increased from 5 billion to 17.5 billion kWh [7]. In view of the serious electric quantity loss, how to avoid or fully utilize water spillage is one of the hot issues faced by hydropower scheduling in China.

Simultaneously, with the rapid development of the Chinese economy, the peak–valley difference in power loads has increased sharply, leading to increased operational costs and operation risks for power systems [8]. The large-scale input of fluctuating and intermittent energy sources (such as wind power and solar power), which are not adjustable, further intensifies the peak-shaving pressure [9,10]. The maximum peak–valley difference in large and medium-sized cities is approximately 50% of the maximum load. Hydropower, which is characterized by rapid load tracking and flexible regulation, is a high-quality peak-shaving power supply [11]. Generally, peak shaving is achieved by the hydropower plants with good regulation performance. In fact, for hydropower plants with poor regulation performance, adjusting the water spillage volume at different periods during the wet season can also achieve a better peak-shaving effect. This paper mainly studies the impact of the strategy of adjusting water spillage on peak shaving.

Actually, short-term hydropower system peak-shaving scheduling is a challenging problem due to the complex solution of the objective function and the consideration of the grid, reservoir, and unit constraints. Studies of this problem have received much attention. Simopoulos et al. [12] proposed an enhanced peak-shaving method to solve the hydro sub-problem, resulting in a modified load curve. Xie et al. [13] used the peaking demands as constraints to improve the benefit maximization model. Su et al. [14] formulated a short-term peak-shaving model for cascaded hydropower plants to

satisfy the complex demand for the scheduling of grid-connected units. The problems of multiple-grid peak shaving were studied, and several methods were proposed to implement different peak-shaving requirements [15–17]. The aforementioned studies can relieve the peak-shaving pressure, but there are still some limitations.

Most studies directly solve the peak-shaving objective function and rarely analyze the peak–valley characteristics of the load curve, sometimes leading to convergence failure. To avoid the above problem, we first accurately divide the peak and valley periods of the load curve before solving the peak-shaving objective function. The division of peak and valley periods based on subjective experience alone is accompanied by human error and, therefore, a more accurate division method is needed. Peak and valley periods have certain aggregation characteristics according to different load values, suitable for division by cluster analysis, which classifies the given data into similar overlapping or non-overlapping groups [18]. Since the dividing line between peak and valley periods is blurred, it is more suitable to use fuzzy cluster analysis (FCA) for automatic identification, which has been widely applied in the field of meteorology, and computer networks [19–21].

Moreover, the existing studies mostly focus on peak shaving during the dry season and wet season without water spillage. In fact, when the incoming water during the wet season is relatively large, for HSCHPs with poor regulation performance, water spillage is unavoidable. HSCHPs usually give priority to economic benefits and mostly aim at increasing power generation during the wet season. Therefore, we consider improving the peak-shaving effect of HSCHPs by adjusting the water spillage volume at each period without significantly affecting the power generation. In this paper, a spillage adjustment strategy called the strategy of releasing water spillage in advance (SRSA) is proposed to increase the power output during peak periods by reducing water spillage.

Mathematically, the short-term scheduling problem of cascaded hydropower plants can be classified as a complex constrained optimization problem with high dimensionality, nonconvexity, nonlinearity, and spatiotemporal coupling [22,23]. Moreover, various methods have been developed to solve this type of problem, including dynamic programming and its improved algorithms [24–26], and heuristic algorithms [27–30]. Dynamic programming suffers from the well-known "curse of dimensionality" as the problem scale expands [31] and is generally not used to solve peak-shaving models. The improved algorithms rely on their initial solutions [32]. Heuristic algorithms are easy to converge to a local optimal or even an infeasible solution and extremely rely on the selection of parameters [33]. In recent years, mixed-integer linear programming (MILP) has gained increasing popularity in the area of hydropower scheduling due to the availability of better performing and more user-friendly commercial software. MILP has powerful functions for processing mathematical models, and binary variables are introduced to linearize complex nonlinear constraints [34]. Given the sensitive hydraulic connections and complex water spillage constraints in HSCHPs, MILP is selected to solve the short-term peak-shaving scheduling problem.

In the short-term peak-shaving model of HSCHPs, there are some nonlinear constraints which are difficult to solve directly with MILP. Piecewise linearization is commonly used to deal with nonlinear constraints by MILP. Most nonlinear constraints can be linearized directly, and the more difficult one is the hydropower output function, which is a nonconvex two-dimensional function. The piecewise linear approximation of this function is achieved in two ways: using a set of one-dimensional functions for approximation or using meshing and triangulation techniques. Unfortunately, the calculation accuracy of the former is insufficient, and the solution efficiency of the latter is affected because many binary variables are introduced [4,35,36]. Considering the computational accuracy and burden, we follow the basic idea in [37] and replace constraints with binary variables with a special ordered set of type two (SOS2), i.e., a set of variables of which at most two can be nonzero and these two variables must be adjacent in the order given to the set [38].

This paper focuses on proposing a novel short-term peak-shaving method considering load characteristics and water spillage for the peak-shaving operation of HSCHPs with water spillage. In brief, the method has three features: (1) FCA is used instead of subjective experience to divide

peak and valley periods of the load curve before directly solving the peak-shaving objective function; (2) SRSA is proposed to improve the peak-shaving ability of HSCHPs with water spillage by discarding water during peak periods in advance; and (3) the hydropower output function is approximated by the meshing technique combined with SOS2 to develop a model-based MILP for determining the optimal scheduling program.

2. Model Formulation

2.1. Objective Function

The purpose of peak shaving in hydropower plants is to smooth the residual load, permitting other power plants which are much less able to respond to sudden changes in electrical demand, such as coal-fired plants, to assume a more stable load. Peak-shaving models mostly use the minimum variance of the residual load series as the objective function [39]. However, this function is nonlinear and difficult to transform via linearization using a piecewise linear approximation. Hence, an alternative form with the minimum variance of the residual load series is adopted in this model, as follows:

$$\min F = \frac{1}{T} \sum_{t=1}^{T} |Re_t - Rem| \tag{1}$$

$$Re_t = C_t - \sum_{d=1}^{D} N_{d,t} \tag{2}$$

$$Rem = \frac{1}{T} \sum_{t=1}^{T} Re_t \tag{3}$$

where T is the total number of periods; t is the period index, $t = 1, 2, \ldots, T$; D is the total number of plants; d is the plant index, $d = 1, 2, \ldots, D$; C_t and Re_t are the original load and residual load during period t (MW), respectively; Rem is the mean of the residual load (MW); and $N_{d,t}$ is the power output of plant d during period t (MW).

Indeed, Equation (1) is still nonlinear and difficult to solve directly using current commercial software. Thus, ancillary variables, defined as follows, are introduced to convert Equation (1).

$$Re_t - Rem \le Raxu_t \tag{4}$$

$$Rem - Re_t \le Raxu_t \tag{5}$$

where $Raxu_t$ is the auxiliary variable during period t (MW).

Then, the objective function can be formulated as follows:

$$\min F = \frac{1}{T} \sum_{t=1}^{T} Raxu_t \tag{6}$$

The above function is just a modification of the minimum variance of the residual load series, which is essentially the same.

2.2. Constraints

(1) Forebay water level, power generation outflow, water release, and power output limits:

$$Z_{d,t}^{\min} < Z_{d,t} < Z_{d,t}^{\max} \tag{7}$$

$$Q_{d,t}^{\min} < Q_{d,t} < Q_{d,t}^{\max} \tag{8}$$

$$U_{d,t}^{\min} < U_{d,t} < U_{d,t}^{\max} \tag{9}$$

$$N_{d,t}^{\min} < P_{d,t} < N_{d,t}^{\max} \tag{10}$$

where $Z_{d,t}^{\min}$ and $Z_{d,t}^{\max}$ are the minimum and maximum forebay water levels of plant d during period t (m^3), respectively; $Q_{d,t}^{\min}$ and $Q_{d,t}^{\max}$ are the minimum and maximum power generation outflows of plant d during period t (m^3/s), respectively; $U_{d,t}^{\min}$ and $U_{d,t}^{\max}$ are the minimum and maximum water releases of plant d during period t (m^3/s), respectively; and $N_{d,t}^{\min}$ and $N_{d,t}^{\max}$ are the minimum and maximum power outputs of plant d during period t (MW), respectively.

(2) Initial and terminal forebay water levels:

$$Z_{d,1} = Z_{d,initial} \tag{11}$$

$$Z_{d,T+1} = Z_{d,terminal} \tag{12}$$

where $Z_{d,initial}$ and $Z_{d,terminal}$ are the initial and terminal forebay water levels of plant d (m), respectively.

(3) Hydraulic connection for a cascaded system:

$$TI_{d,t} = U_{d-1,t-\tau_d} + NI_{d,t} \tag{13}$$

where $TI_{d,t}$ and $NI_{d,t}$ are the total inflow and natural inflow of plant d during period t (m^3/s); $U_{d,t}$ is the water release of plant d during period t (m^3/s); and τ_d is the water delay, i.e., the time until the discharge of upstream plant d-1 reaches downstream plant d (h).

(4) Continuity balance equation:

$$V_{d,t+1} = V_{d,t} + 3600 \times \left(TI_{d,t} - U_{d,t} \right) \times \Delta t \tag{14}$$

where $V_{d,t}$ and $V_{d,t+1}$ are the storage of plant d at the beginning of period t and at the end of period t (m^3), respectively; and Δt is the time interval (h).

(5) Water release equation:

$$U_{d,t} = Q_{d,t} + S_{d,t} \tag{15}$$

where $S_{d,t}$ is the water spillage of plant d during period t (m^3/s).

(6) Ecological flow constraint:

$$Q_{d,t} \geq EF_{d,t} \tag{16}$$

where $EF_{d,t}$ is the ecological flow of plant d during period t (m^3/s).

(7) Net water head equation:

$$H_{d,t} = \left(Z_{d,t} + Z_{d,t+1} \right)/2 - ZT_{d,t} - \Delta H_{d,t} \tag{17}$$

where $H_{d,t}$ is the net head of plant d during period t (m); $Z_{d,t}$ and $Z_{d,t+1}$ are the forebay water levels of plant d at the beginning of period t and at the end of period t (m), respectively; $ZT_{d,t}$ is the tailrace water level of plant d during period t (m); and $\Delta H_{d,t}$ is the head loss of plant d during period t (m).

(8) Hydropower output function:

$$N_{d,t} = f_d^{NQH}\left(Q_{d,t}, H_{d,t} \right) \tag{18}$$

(9) Relationship between storage and forebay water level:

$$V_{d,t} = f_d^{ZV}\left(Z_{d,t} \right) \tag{19}$$

(10) Relationship between tailrace water level and water release:

$$ZT_{d,t} = f_d^{ZU}\left(U_{d,t}\right) \tag{20}$$

(11) Relationship between head loss and power generation outflow:

$$\Delta H_{d,t} = f_d^{HQ}\left(Q_{d,t}\right) \tag{21}$$

3. Methods

3.1. Automatically Dividing Peak and Valley Periods via FCA

Peak and valley membership determines the correlation between the load at a certain period and the peak and valley loads of the day, regardless of the specific load at this period. The day is divided into T periods and the periods are recorded as $\{1, \ldots, t, \ldots T\}$, and the corresponding load values are $\{p_1, \ldots, p_t, \ldots p_T\}$. As presented in Equations (22) and (23), the large semitrapezoid membership function determines the membership d_{ft} of the load during period t corresponding to the peak load, and the membership d_{gt} of the load during period t corresponding to the valley load is determined by the small semitrapezoid membership function [40].

$$d_{ft} = \frac{(p_t - p_{\min})}{(p_{\max} - p_{\min})} \tag{22}$$

$$d_{gt} = \frac{(p_{\max} - p_t)}{(p_{\max} - p_{\min})} \tag{23}$$

where $p_{\max}$ and $p_{\min}$ are the maximum and minimum loads over all periods, respectively.

FCA is mainly divided into the following steps.

Step 1: Establish and standardize a peak–valley membership matrix.

Use the peak and valley membership of each period $m_t = \left(d_{ft}, d_{gt}\right)$ as the statistical index to obtain a peak–valley membership matrix $M = (m_t)_{t \in T}$ and standardize M according to Equation (24) to get a standardized peak–valley membership matrix $M^* = \left(m_t^*\right)_{t \in T}, m_t^* = \left(d_{ft}^*, d_{gt}^*\right)$.

$$d_{kt}^* = \frac{d_{kt} - \dfrac{1}{T}\displaystyle\sum_{t=1}^{T} d_{kt}}{\sqrt{\dfrac{1}{T}\displaystyle\sum_{t=1}^{T}\left(d_{kt} - \dfrac{1}{T}\displaystyle\sum_{t=1}^{T} d_{kt}\right)^2}}, k = f, g \tag{24}$$

Step 2: Establish a fuzzy similarity matrix.

Determine the similarity r_{xy} of m_x^* and m_y^* by Equation (25), and construct a fuzzy similarity matrix $R = \left(r_{xy}\right)_{T \times T}$.

$$r_{xy} = \begin{cases} 1 & x = y \\ 1 - c\left(\left|d_{fx}^* - d_{fy}^*\right| + \left|d_{gx}^* - d_{gy}^*\right|\right) & x \neq y \end{cases} \tag{25}$$

where c is a constraint variable; $x = 1, 2, \ldots T$; and $y = 1, 2, \ldots T$.

Step 3: Dynamic clustering based on a fuzzy equivalent matrix.

R is squared in turn, i.e., $R \to R^2 \to R^4 \to R^8 \to \cdots$. When $R^{2n} = R^n \circ R^n = R^n$ appears for the first time, $R^* = R^n$ is the required fuzzy equivalent matrix (transitive closure), which is expressed as $R^* = \left(w_{xy}\right)_{T \times T}, 0 \leq w_{xy} \leq 1$.

$$R \circ R = \max\left(\min\left(R_{xl}, R_{yl}\right), R_{xy}\right) \tag{26}$$

where $l = 1, 2, \ldots T$.

Let λ equal any element value in R^* (from maximum to minimum) to obtain the λ truncation matrix R_λ^* of R^*.

$$R_\lambda^* = \left(w_{xy}(\lambda) \right)_{T \times T} \tag{27}$$

where

$$w_{xy}(\lambda) = \left\{ \begin{array}{ll} 1 & w_{xy} \geq \lambda \\ 0 & w_{xy} < \lambda \end{array} \right. \qquad \lambda \in [0, 1] \tag{28}$$

The column vector of R_λ^* corresponds to the element in $\{p_1, \ldots, p_t, \ldots p_T\}$. When some elements in $\{p_1, \ldots, p_t, \ldots p_T\}$ are of the same type, the corresponding column vector in R_λ^* must be equal. As λ decreases from maximum to minimum, dynamic clustering is performed.

Step 4: Threshold determination.

Actually, λ is gradually reduced from 1 for dynamic clustering until the number of clusters is 3, and the automatic division results for the peak, flat, and valley periods are obtained. In practical applications, the peak, flat, and valley periods' durations should be generally not less than 2 h.

3.2. Strategy of Releasing Water Spillage in Advance(SRSA)

Currently, HSCHPs mainly pursue the power generation benefit and often generate water spillage when the incoming water is particularly large during the wet season due to poor regulation performance. The amount of water spillage can be controlled by the gate. Simultaneously, the short-term scheduling of the power grid is faced with huge peak-shaving pressure because of the shape of the peak–valley difference. It is necessary to reasonably utilize the water spillage of HSCHPs to obtain greater peak-shaving benefits during the wet season. Therefore, SRSA is proposed to increase the power output during peak periods by reducing the water spillage during peak periods.

According to the principle of water balance, when the forebay water levels at the beginning and end of the scheduling period are fixed and the incoming water is determined, the water release during the scheduling period is also fixed. In the actual scheduling (AS) of HSCHPs during the wet season, water at each period is generally released evenly to generate electricity. For HSCHPs, to improve the power generation benefit, whether it is the dry season or wet season, it is necessary to place the operating water level near the highest position because the power generation heads are the largest and the power generation is also the largest under the same incoming water condition. To improve the peak-shaving benefit, the proposed SRSA is to release more water during valley periods, thereby reducing the water release during peak periods. Judging by the relationship between the water release and the tailrace water level, the tailrace water levels are also reduced, resulting in an increase in the power generation heads, thereby increasing the power output during peak periods.

The adjustment process of SRSA is shown in Figure 2. SRSA is a further adjustment based on the water spillage results of AS. In SRSA, the concept of the water spillage ratio (WSR) is introduced, i.e., the ratio of water spillage that is released in advance to the original total water spillage in a certain period. For plant b, after redistributing the water spillage, the water spillage during valley periods consists of two parts: the original water spillage ("B") and the water spillage from the peak periods ("A"); WSR is equal to A/C. Under the condition of constant power generation outflow, during valley periods, the power output of plant b decreases due to the increased tailrace water levels. In other words, part of the power output of plant b during valley periods is sacrificed in exchange for the increased power output during peak periods, thereby alleviating the peak period pressure. According to the water release of plant b after adopting SRSA, the optimal water spillage of plant b that makes the objective function relatively optimal can be calculated without making changes to other plants. When the water release of plant b is known (the water spillage and power generation outflow are known), the total inflow of plant $b + 1$ is determined and the water release can also be obtained. The same operation is performed on plant $b + 1$ to calculate the optimal water spillage of plant $b + 1$.

After adjusting the water spillage of all plants, the optimal spillage adjustment program is determined so that the power output results of all plants are obtained.
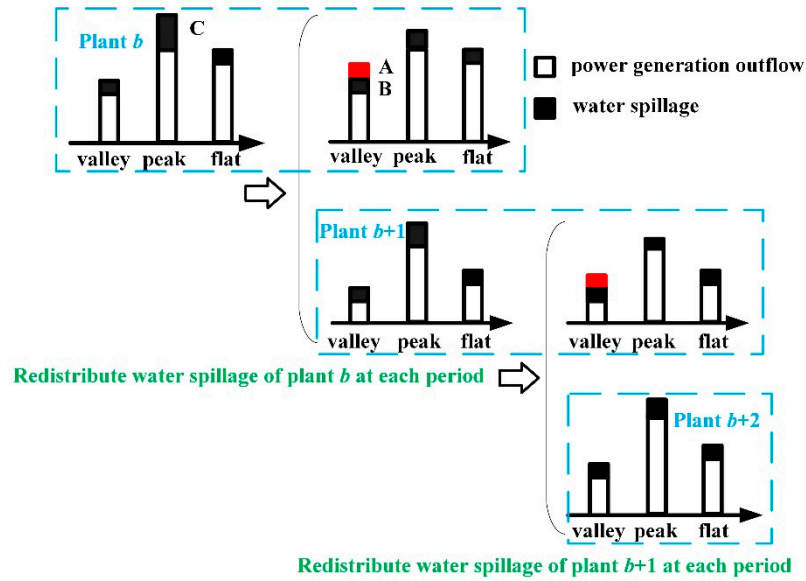

Figure 2. Adjustment process of the spillage adjustment strategy.

In the proposed strategy, there is no change to the water release during flat periods. The reasons are as follows: first, if more water is released during valley periods, the power output during valley periods will be further reduced, affecting the daily total power generation; and second, limited by the reservoir storage and tailrace water level, the water that can be released during valley periods is certain, meaning that if SRSA is also carried out during flat periods, the water spillage from the peak periods may be reduced.

3.3. Steps for SRSA

The SRSA for HSCHPs should be carried out from the upstream plant to the downstream plant, according to the following process:

Step 1:   The plant currently being adjusted for water spillage is recorded as b, and the total number of plants with water spillage is recorded as B.

Step 2:   The most upstream plant $b = 1$, and its original water spillage is recorded as $WS_{b,t}^*, t \in T$ (obtained from AS).

Step 3:   For plant b, divide the peak periods' water spillage equally into the valley periods according to Equation (29) to calculate the adjusted water spillage, $WS_{b,t}, t \in T$, and the original water spillage of plant $b + 1$, $WS_{b+1,t}^*, t \in T$, by the proposed model.

Step 4:   If $b < B$, $b = b + 1$ and jump to Step 3, otherwise go to Step 5.

Step 5:   End the adjustment process.

$$
\begin{cases}
WS_{b,t} = WS_{b,t}^* + extra & t \in T_{valley} \\
WS_{b,t} = WS_{b,t}^* & t \in T_{flat} \\
WS_{b,t} = (1 - \varepsilon_t) \times WS_{b,t}^* & t \in T_{peak}
\end{cases}
\tag{29}
$$

$$
extra = \frac{\sum\limits_{t \in T_{peak}} \varepsilon_t \times WS_{b,t}}{total}
\tag{30}
$$

where $WS_{b,t}^*$ and $WS_{b,t}$ are the water spillage of plant b during period t before and after adjusting the water spillage, respectively; T_{peak}, T_{flat}, and T_{valley} are the peak, flat, and valley periods, respectively; *extra* is the extra water spillage for each valley period; *total* is the sum of the number of valley periods; and ε_t is the WSR during period t, $t \in T_{peak}$, i.e., the ratio of water spillage released in advance to the total water spillage during period t. In principle, the value range of ε_t is $[0, 1]$, but in fact, its range depends on the reservoir storage and tailrace water level limits of the plants. The optimal ε_t can be calculated by the optimization model.

3.4. Linearization of Hydropower Output Function Based on SOS2

There are some nonlinear constraints, most of which can be achieved by simple linear equations, such as the relationship between the storage and forebay water level, the relationship between the tailrace water level and water release, and the relationship between the head loss and power generation outflow, in the short-term peak-shaving scheduling of HSCHPs with poor regulation performance. In particular, the hydropower output function is a typical nonconvex, nonlinear two-dimensional function, which is troublesome to linearize. In this paper, the meshing technique combined with SOS2 is used to linearize the hydropower output function since special ordered sets are well used in the linearization of the two-dimensional function [41]. As Figure 3a shows, the hydropower output function in Equation (18) is represented by grid values by discretizing the water head H into I points from the maximum to the minimum $\{H_i^*\}_{i \in I}$ and the power generation outflow Q into J points from the maximum to the minimum $\{Q_j^*\}_{j \in J}$. The non-negative auxiliary variable $\delta_{i,j}$ in Figure 3b is used as the weight of the power output $N_{i,j}^* = f^{NHQ}\left(H_i^*, Q_j^*\right)$ in Figure 3a.
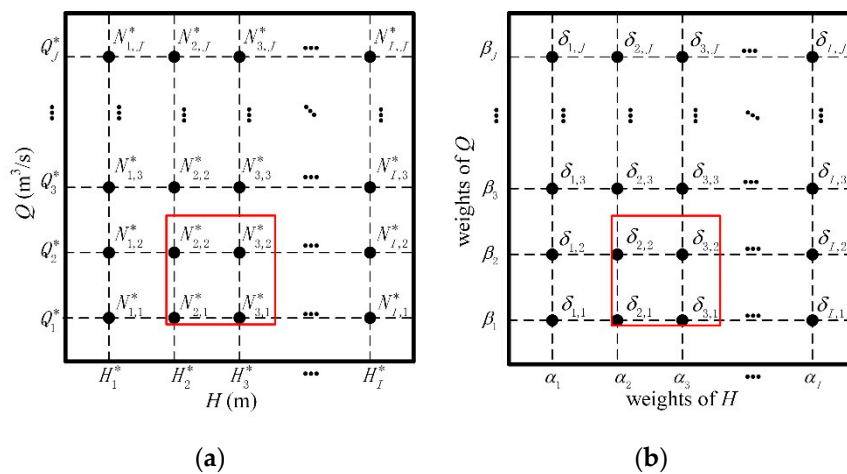

Figure 3. Linearization sketch of the hydropower output function. (**a**) Discretization of the hydropower output function; (**b**) weights of discretized values.

The specific modeling is as follows:

$$\sum_{i \in I} \sum_{j \in J} \delta_{i,j} = 1, \delta_{i,j} \geq 0 \tag{31}$$

$$\alpha_i = \sum_{j \in J} \delta_{i,j}, \forall i \in I \tag{32}$$

$$\beta_j = \sum_{i \in I} \delta_{i,j}, \forall j \in J \tag{33}$$

$$\sum_{i \in I} \alpha_i H_i^* = H \tag{34}$$

$$\sum_{j \in J} \beta_j Q_j^* = Q \tag{35}$$

$$\sum_{i \in I} \sum_{j \in L} \delta_{i,j} N_{i,j}^* = N \tag{36}$$

where sets $\{\alpha_1, \alpha_2, \ldots, \alpha_I\}$ and $\{\beta_1, \beta_2, \ldots, \beta_J\}$ are SOS2 sets, which do not increase the number of variables.

Equations (34)–(36) express the point (H, Q, N) as a convex combination of $G^3 = \{G_{i,j}\}_{i \in I, j \in J}$ and $G_{i,j} = \left(H_i^*, Q_j^*, N_{i,j}^* \right)$. According to the characteristics of SOS2 (at most, two variables in the set are nonzero and they must be adjacent), only four neighboring grid points can be nonzero and the point (H, Q, N) is confined to the interior of these four spatial grids. As shown in Figure 3b, for instance, $\delta_{2,1}$, $\delta_{2,2}$, $\delta_{3,1}$, and $\delta_{3,2}$ are nonzero, while all others are zero, meaning that only $N_{2,1}^*$, $N_{2,2}^*$, $N_{3,1}^*$, and $N_{3,2}^*$ are nonzero in Figure 3a. When the number of rasterized grid points is sufficient, the point (H, Q, N) will infinitely approach the given output function surface.

3.5. Overall Solution Process

To reduce the peak–valley difference, a novel peak-shaving method considering load characteristics and water spillage for the peak-shaving operation of HSCHPs with water spillage is proposed. The overall solution process of the proposed method is presented in Figure 4. First, the automatic division of peak and valley periods is carried out by FCA, i.e., the green line in Figure 4. Then, the linearization of the model is achieved by the meshing technique combined with SOS2. Final, the optimal scheduling results are obtained to achieve an improved peak-shaving effect by SRSA, i.e., the blue line in Figure 4. The model presented in the previous section is solved with Lingo (17.0 × 64), a modeling language widely used for optimal scheduling.
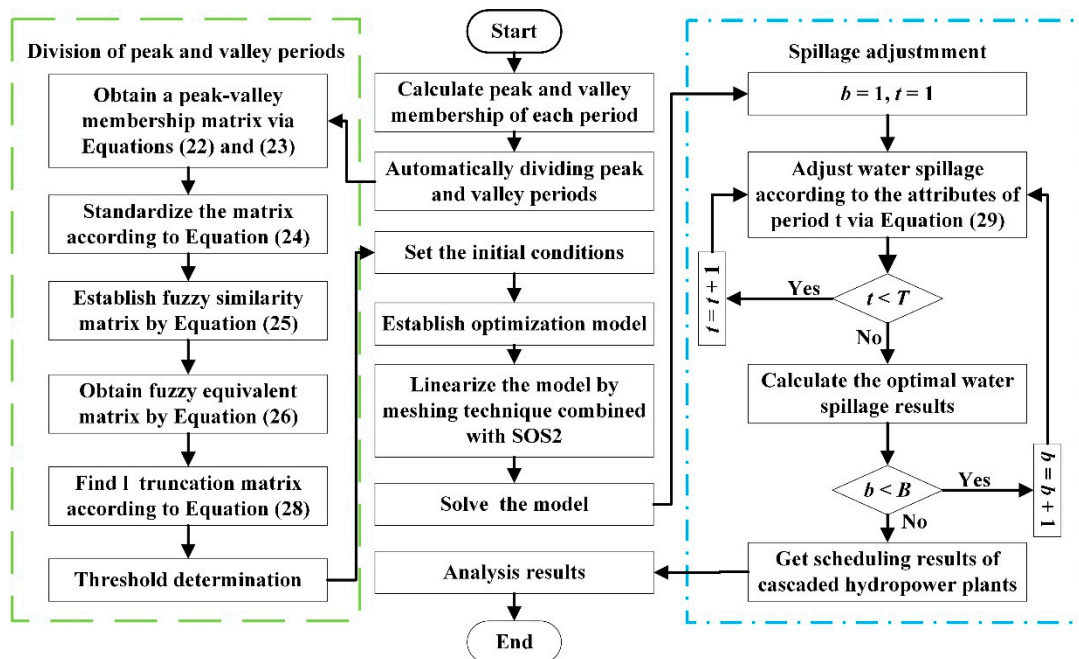

Figure 4. Overall solution process; SOS2 is a special ordered set of type two, T is the total number of periods, t is the period index, B is the total number of plants, and b is the plant index.

4. Application in the Hongshui River Basin

The Hongshui River, one of the first thirteen hydropower bases in China, is located in the upper reaches of the Xijiang River in the Pearl River Basin, with a total length of 1050 km. The total fall and annual average water volume are 760 m and 130 Gm^3, respectively, meaning rich hydropower resources. There are 10 hydropower plants that are expected to be built in the Hongshui River, including 1 multiyear regulating hydropower plant, 2 annually regulating hydropower plants, 6 daily regulating hydropower plants, and 1 run-of-river hydropower plant. Currently, all hydropower plants except Datengxia are operational and generating some quantity of water spillage.

Pingban and the cascaded system consisting of Dahua, Bailongtan, Letan, and Qiaogong were selected as study cases to test the feasibility and validity of the proposed method, as shown in Figure 1. Table 1 lists the boundary conditions of the selected plants.

Table 1. Boundary conditions.

Items	Pingban	Dahua	Bailongtan	Letan	Qiaogong
Maximum forebay water level (m)	440.00	155.00	130.00	112.00	84.00
Minimum forebay water level (m)	437.50	153.00	127.00	111.00	82.00
Maximum storage (Mm^3)	211.76	393	86.3	402	191
Minimum storage (Mm^3)	184.42	356	73.7	356	164
Maximum generation flow (m^3/s)	1320	3076	2580	3432	3680
Ecological flow (m^3/s)	62	189	190	209	214
Maximum output of plant (MW)	405	566	192	600	456
Minimum output of plant (MW)	200	320	90	280	150
Constant delay time (h)	/	/	2	5	2
Natural inflow (m^3/s)	/	/	0	171	0

In this paper, the initial and terminal forebay water levels of each hydropower plant were set at the maximum to obtain as much power generation benefits as possible in the current scheduling period and the next scheduling period.

When each selected power plant releases water according to its maximum generation flow value, the time required for the reservoir storage from maximum to minimum is listed in Table 2. The adjustable storage is the difference between the maximum storage and minimum storage. Obviously, when each selected hydropower plant generates electricity at the maximum generation flow without considering the incoming water, the forebay water level falls from the maximum to the minimum within a few hours, demonstrating that the forebay water level is quite sensitive during the scheduling period. In other words, the selected plants are all head-sensitive hydropower plants.

Table 2. Time required for reservoir storage from maximum to minimum.

Items	Pingban	Dahua	Bailongtan	Letan	Qiaogong
Adjustable storage (Mm^3)	27.34	37	12.6	46	27
Time (h)	5.75	3.34	1.36	3.72	2.04

5. Results and Discussion

5.1. Identification of Peak, Flat, and Valley Periods

Since Hongshui River enters the wet season in July, HSCHPs' incoming water is abundant, accompanied by serious water spillage and blocked head problems. Consequently, one day in July with a large amount of steady incoming water (to make the results more intuitive) was selected. The peak–valley difference is 22,966.08 MW, accounting for approximately 32% of the maximum load during the day. The valley periods must be identified before the use of SRSA. FCA, in which $c = 0.1$,

was chosen to divide the peak, flat, and valley periods. From Figure 5a, the number of clusters is 3 when λ is reduced to 0.9451. Periods 10–22 are peak periods; periods 7–9 and 23–24 are flat periods; and periods 1–6 are valley periods. The classification results satisfy the requirement that the peak, flat, and valley periods are not less than 2 h.
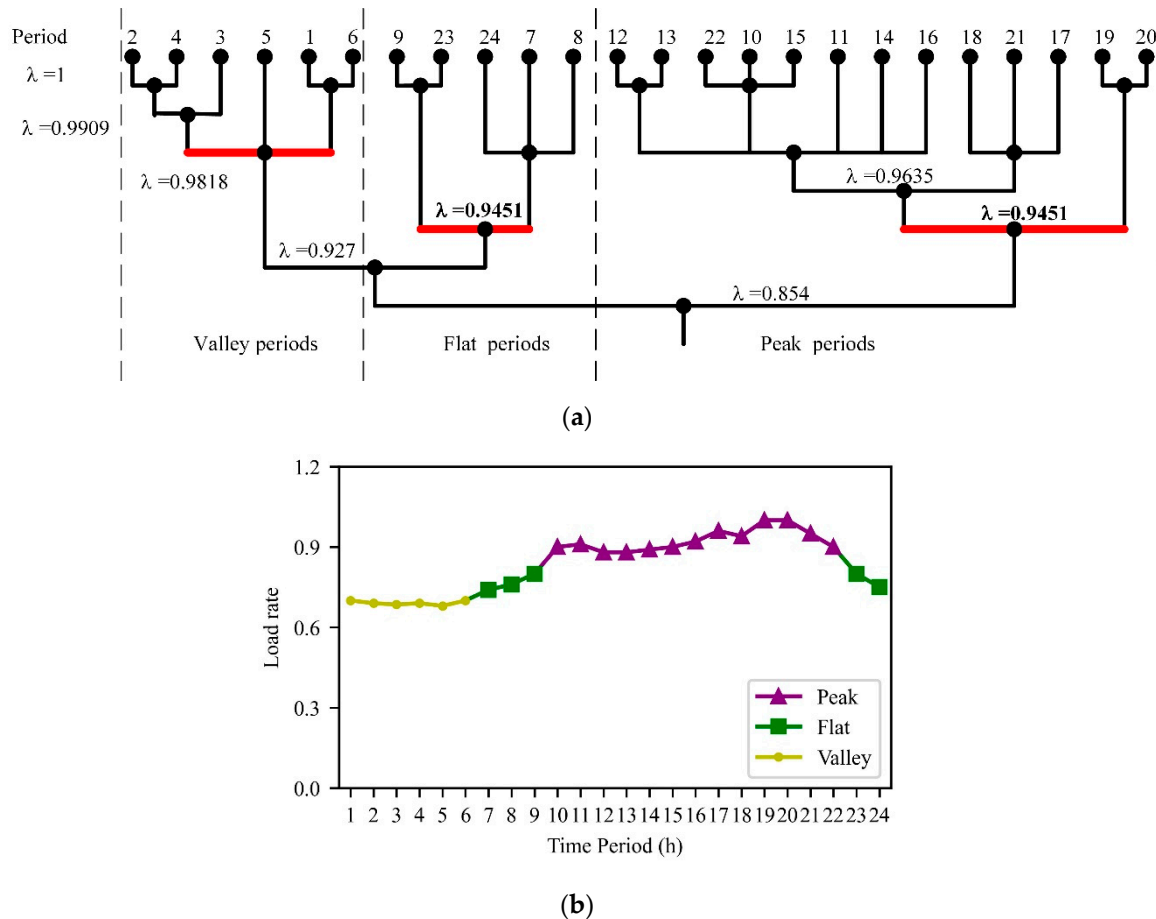

(**a**)

(**b**)

Figure 5. Identification of peak, flat, and valley periods. (**a**) Dynamic clustering graph; (**b**) division results of peak, flat, and valley periods.

5.2. Case 1—Single Plant

Before verifying whether the short-term peak-shaving method was helpful for cascaded hydropower plants, a single hydropower plant was tested to show how the method works. In order to show the advantages of the proposed method, the scheduling with the proposed method (SPM), AS, and scheduling achieved only by solving the objective function (SAF) were compared. The initial and final forebay water levels and the incoming water are determined, therefore, the water release is certain. Thus, the ratio of water spillage to water release was used to indicate the total water spillage volume of the plant.

Pingban, a typical daily regulating hydropower plant, was selected to prove the effectiveness of SPM. Table 3 presents the results of the SPM, AS, and SAF of Pingban. As shown in Table 3, compared to AS, the peak-shaving capacity of SPM increased from 0 to 39.81 MW (9.8% of the installed capacity), and the object value of SPM decreased from 7075.97 to 7064.21 MW. Moreover, the ratio of water spillage to water release of SPM was consistent with that of AS, showing that SPM did not add additional water spillage. Compared to AS, SPM lost part of the daily total power generation, but SAF lost more. Although the peak-shaving capacity of SAF was greater than that of SPM, it sacrificed more daily total power generation and added extra water spillage (27.1%). In comparison, SPM achieved a

certain peak-shaving effect while preserving more power generation and did not generate additional water spillage, which was more in line with an economic operation.

Table 3. Comparison results of Pingban on scheduling with the proposed method (SPM), actual scheduling (AS), and scheduling achieved only by solving the objective function (SAF); WSR = water spillage ratio.

Items	SPM	AS	SAF
Daily total power generation (10^4 kWh)	830.73	839.08	684.09
Peak period power generation (10^4 kWh)	464.09	454.50	464.09
Peak-shaving capacity (MW)	39.81	0	160.08
Object value (MW)	7064.21	7075.97	6998.02
Ratio of water spillage to water release (%)	10.8	10.8	27.1
Average of WSRs (%)	100	/	/

The results of SPM and AS are compared in Figure 6. By SRSA, the water spillage during peak periods (periods 10–22) was reduced, that of the valley periods (periods 1–6) was increased, and that of the flat periods (periods 7–9 and periods 23–24) was unchanged, reflected in Figure 6b. Since the power generation outflow was unchanged, the change trend of water release is the same as that of water spillage. The water release during each period met the ecological flow constraint.
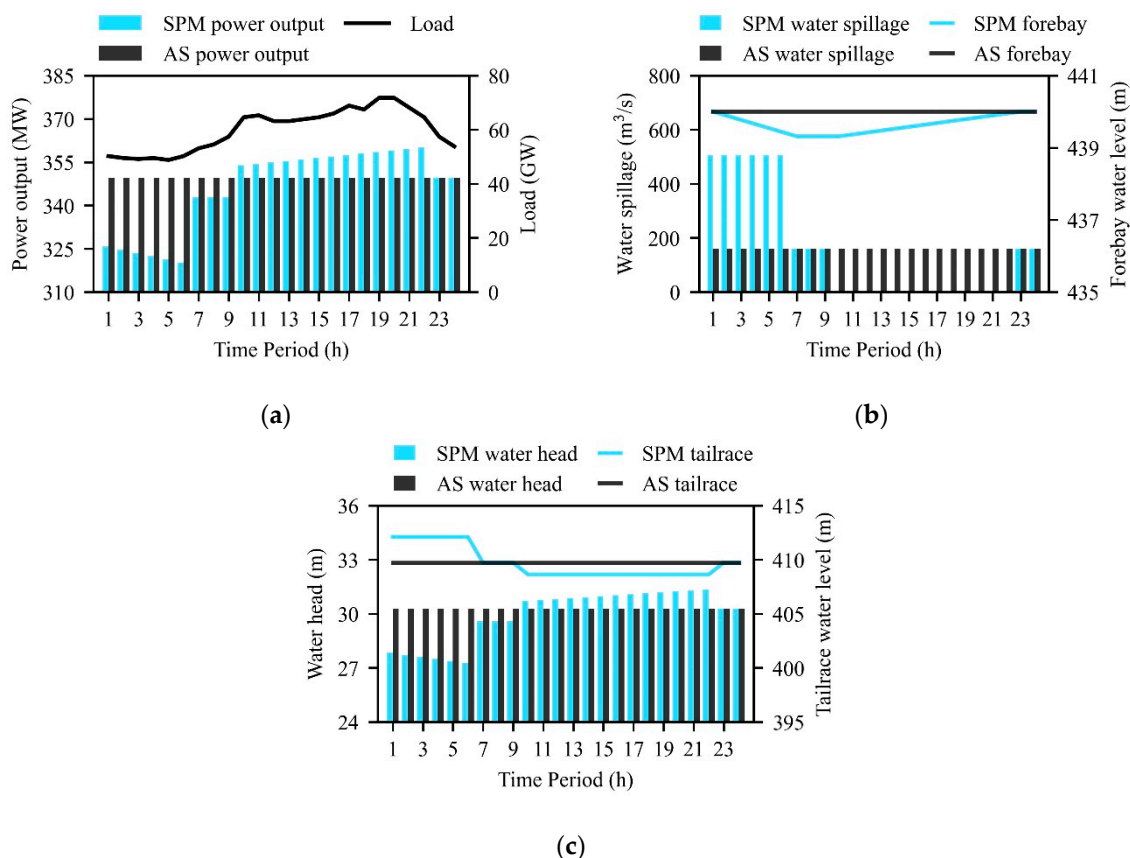

(**a**)

(**b**)

(**c**)

Figure 6. The results of SPM and AS. (**a**) Power output; (**b**) water spillage and forebay water level; (**c**) tailrace water level and water head.

For periods 1–6, as more water was released, the tailrace water levels increased and the forebay water levels decreased, leading to decreased water heads; assuming that the power generation outflow was unchanged, the power outputs decreased. Similarly, for periods 11–22, the water release was reduced, thus the tailrace water levels decreased. Although the forebay water levels were not as high as those of AS, the water heads were generally higher, resulting in increased power outputs. As the

forebay water level gradually increased, the water head increased, as did the power output. During flat periods 7–9, although the tailrace water levels were unchanged, since the forebay water levels decreased, the water heads also decreased, leading to decreased power outputs. During flat periods 23–24, the water heads were unchanged, thus the power outputs were also unchanged.

In general, compared to the AS's results, the daily total power generation of SPM decreased, but the peak period power generation increased, and the proportion of the latter in the former increased from 54.2% to 55.9%. For the selected plant, WSR at each peak period was 100%, meaning no water spillage during peak periods.

5.3. Case 2—Cascaded System

A cascaded hydropower system consisting of Dahua, Bailongtan, Letan, and Qiaogong, the HSCHPs in the Hongshui River Basin, was selected to validate the proposed SPM. Table 4 shows the results of the SPM, AS, and SAF of the cascaded system. From Table 4, SPM's peak-shaving capacity of the selected cascade hydropower system was 668.77 MW (36.9% of the total installed capacity), which exceeded AS's (0 MW). The peak-shaving capacity of each plant of SPM increased by 26.0%, 13.6%, 43.8%, and 56.8% of their installed capacity, respectively. SPM's object value (6892.28 MW) was better than AS's (7075.98 MW). The ratio of water spillage to water release of each plant in SPM was the same as that of AS, showing there was not more water spillage in SPM.

Table 4. Comparison results of the cascaded system on SPM, AS, and SAF.

Items		Dahua	Bailongtan	Letan	Qiaogong	Cascade
Daily total power generation (10^4 kWh)	SPM	1129.39	422.40	1082.13	850.75	3484.66
	AS	1183.60	422.40	1089.23	893.43	3588.66
	SAF	1015.94	337.47	1030.02	731.76	3115.19
Peak period power generation (10^4 kWh)	SPM	657.63	237.85	659.45	553.03	2107.97
	AS	641.12	228.80	590.00	483.94	1943.86
	SAF	663.94	238.47	722.02	566.76	2191.19
Peak-shaving capacity (MW)	SPM	146.91	26.06	262.52	258.85	668.77
	AS	0	0	0	0	0
	SAF	226.26	100.76	279.61	288.63	885.87
Object value (MW)	SPM	/	/	/	/	6892.28
	AS	/	/	/	/	7075.98
	SAF	/	/	/	/	6672.58
Ratio of water spillage to water release (%)	SPM	25.0	37.1	19.6	13.8	23.7
	AS	25.0	37.1	19.6	13.8	23.7
	SAF	35.4	50.8	27.3	31.8	31.8
Average of WSRs	SPM	55.8	0	51.4	100	/
	AS	/	/	/	/	/
	SAF	/	/	/	/	/

Compared with SAF, SPM's peak-shaving capacity and object value were not particularly advantageous, but SPM sacrificed smaller daily total power generation. The main reason was that Dahua, Bailongtan, Letan, and Qiaogong in SAF all generated more water spillage. Under the condition that their respective total water release was constant, the increase in water spillage led to a decrease in power generation outflow, which affected the power outputs.

The power output results of SPM and AS for the cascaded hydropower system are illustrated in Figure 7. The cascaded power outputs during periods 1–10 decreased and those during periods 11–24 increased. On the whole, the peak period power generation increased. In general, from AS to SPM, the daily total power generation decreased by 3.3%, but the peak period power generation increased by 8.3%. The proportion of the latter in the former increased from 54.2% to 60.6%.
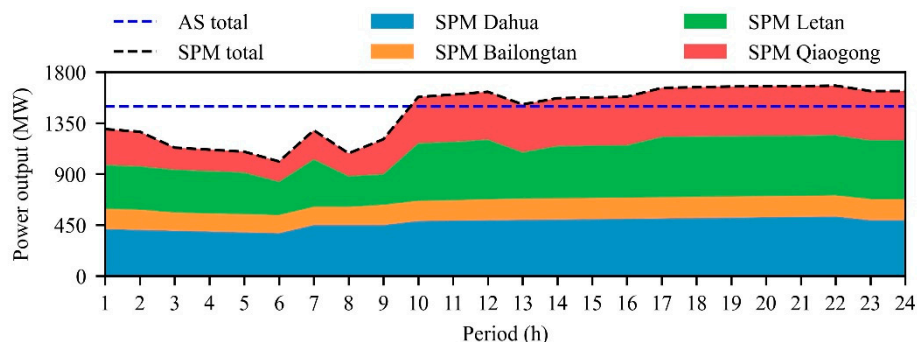
Figure 7. Comparsion of power output results of SPM and AS.

In summary, SPM improved the efficiency of peak regulation without significantly affecting the power generation benefits and generating excess water spillage.

A comparison of water spillage, forebay water levels, water heads, and tailrace water levels between SPM and AS is presented in Figure 8. Dahua, as the most upstream hydropower plant, was only affected by the adjustment of its own water spillage, thus its optimal operating status was similar to that of Case 1. However, Bailongtan, Letan, and Qiaogong were affected by both the water release of the upstream plant and their own water spillage adjustment. When the water release of the upstream plant changed, the impact on the downstream plant was reflected in a change in the inflow. Affected by the time lag, the optimal water spillage of three downstream plants during certain flat and peak periods after adjusting the water spillage was larger than AS's. On the whole, the water spillage in most peak periods of each plant was reduced. Adopting SRSA, although the forebay water level and tailrace water level change trends of each plant in the cascaded system were different, their peak period power generation and peak-shaving capacity both increased, as presented in Table 4. Considering water spillage and power generation outflow, the water discharge during each period of each plant met the ecological flow constraints.

Notably, for Bailongtan, after the water spillage of Dahua was adjusted, the tailrace water levels during peak periods were unsuitable to increase further, limited by the small storage capacity and poor regulation performance. Therefore, the WSRs of Bailongtan during peak periods were 0. Bailongtan was only affected by the water release of the upstream plant.
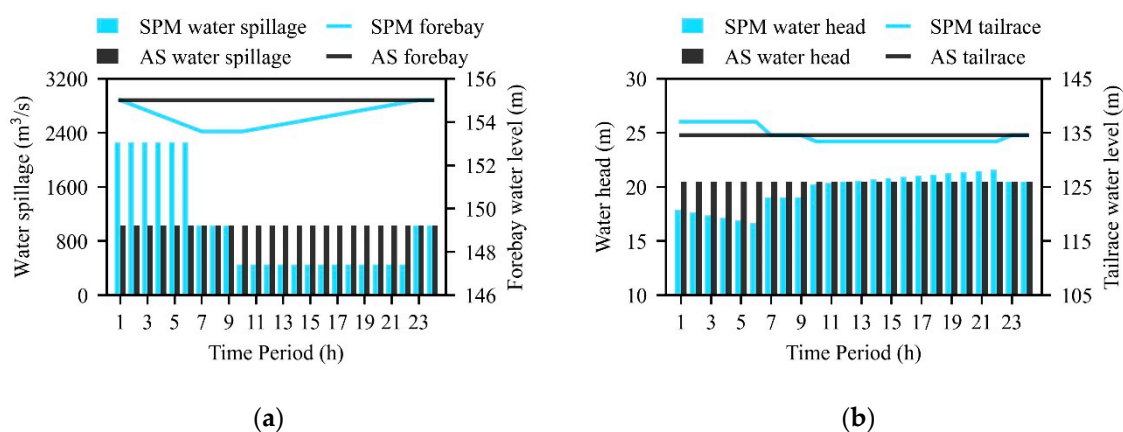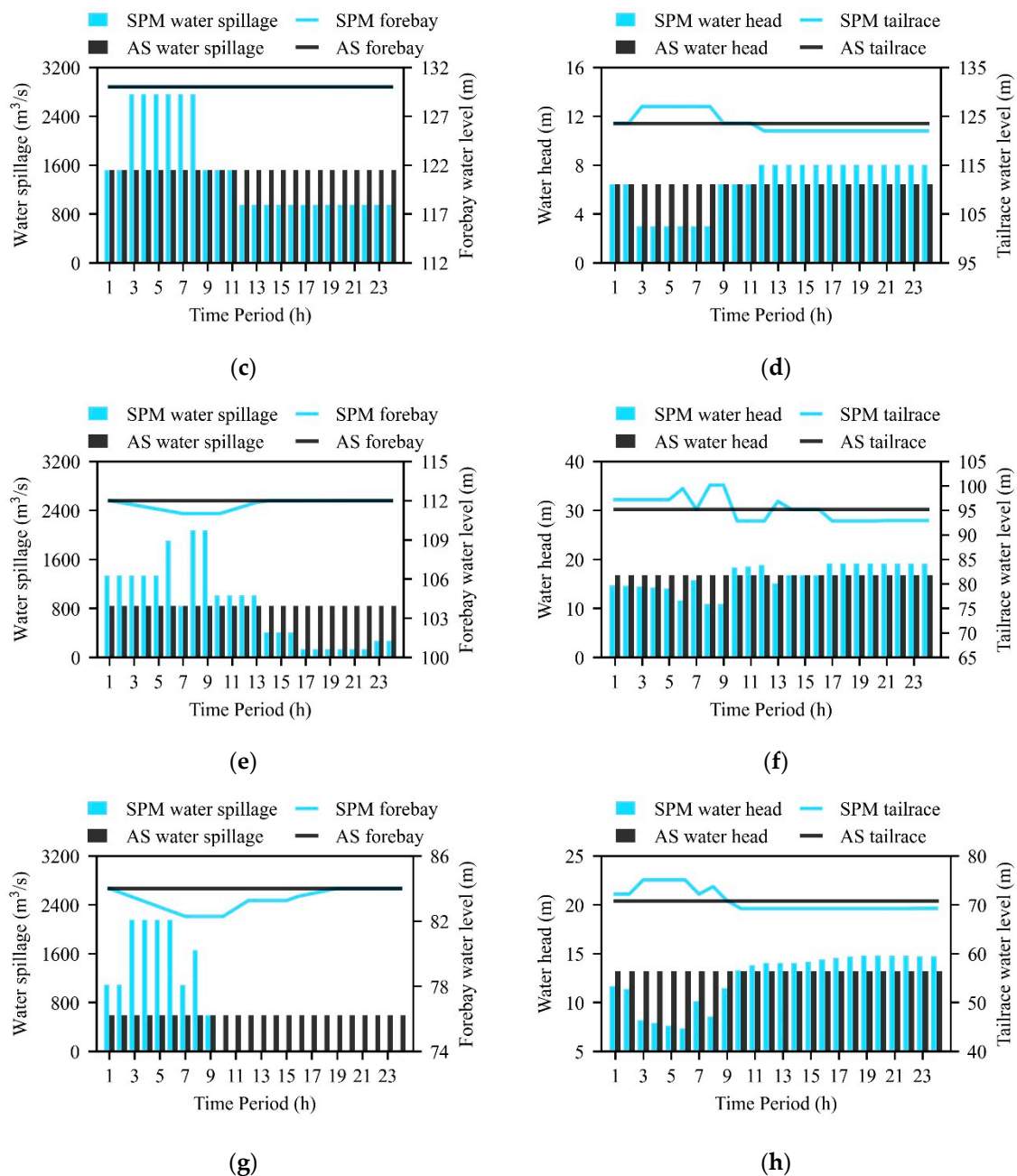

(a)

(b)

Figure 8. *Cont.*

Figure 8. Comparison results of the cascaded system of SPM and AS. (**a**) Pingban water spillage and forebay water level; (**b**) Pingban tailrace water level and water head; (**c**) Bailongtan water spillage and forebay water level; (**d**) Bailongtan tailrace water level and water head; (**e**) Letan water spillage and forebay water level; (**f**) Letan tailrace water level and water head; (**g**) Qiaogong water spillage and forebay water level; (**h**) Qiaogong tailrace water level and water head.

6. Conclusions

With an increasing peak–valley difference of the power load and the continuous production of intermittent energy, such as wind power and solar power, hydropower plants, especially cascaded hydropower plants, are expected to participate in deep peak-shaving scheduling. However, most cascaded hydropower plants are HSCHPs. During the wet season, the large volume of incoming water inevitably produces water spillage. Studying how to utilize water spillage for deep peak shaving of HSCHPs is valuable.

A new short-term peak-shaving method considering load characteristics and water spillage for the peak-shaving operation of HSCHPs is proposed to utilize water spillage to reduce the peak–valley difference and increase the peak-shaving benefits. The HSCHPs in the Hongshui River Basin are used to test the efficiency and quality of the proposed method. The optimization calculation results demonstrate that the peak-shaving method can reduce the peak–valley difference to a certain extent and improve the efficiency of peak regulation without significantly affecting the power generation benefits and generating more water spillage.

References

1. Cheng, C.T.; Yan, L.Z.; Mirchi, A.; Madani, K. China's Booming Hydropower: Systems Modeling Challenges and Opportunities. *J. Water Resour. Plan. Manag.* **2017**, *143*, 02516002. [CrossRef]
2. National Energy Administration. Available online: http://www.nea.gov.cn/2020-01/20/c_138720881.htm (accessed on 10 November 2020).
3. Feng, Z.K.; Niu, W.J.; Cheng, C.T. China's large-scale hydropower system: Operation characteristics, modeling challenge and dimensionality reduction possibilities. *Renew. Energy* **2019**, *136*, 805–818. [CrossRef]
4. Cheng, C.T.; Wang, J.Y.; Wu, X.Y. Hydro Unit Commitment with a Head-Sensitive Reservoir and Multiple Vibration Zones Using MILP. *IEEE Trans. Power Syst.* **2016**, *31*, 4842–4852. [CrossRef]
5. XINHUANET. Available online: http://www.xinhuanet.com/energy/2019-01/30/c_1124061943.htm (accessed on 14 October 2020).
6. ESCN. Available online: http://www.escn.com.cn/news/show-699676.html (accessed on 13 November 2020).
7. SOHU. Available online: https://www.sohu.com/a/231139439_550183 (accessed on 14 October 2020).
8. Ding, N.; Duan, J.H.; Xue, S.; Zeng, M.; Shen, J.F. Overall review of peaking power in China: Status quo, barriers and solutions. *Renew. Sustain. Energy Rev.* **2015**, *42*, 503–516. [CrossRef]
9. Blokhuis, E.; Brouwers, B.; Putten, E.V.D.; Schaefer, W. Peak loads and network investments in sustainable energy transitions. *Energy Policy* **2011**, *39*, 6220–6233. [CrossRef]
10. Wang, X.X.; Virguez, E.; Xiao, W.H.; Mei, Y.D.; Patino-Echeverri, D.; Wang, H. Clustering and dispatching hydro, wind, and photovoltaic power resources with multiobjective optimization of power generation fluctuations: A case study in southwestern China. *Energy* **2019**, *189*, 116250. [CrossRef]
11. Gu, Y.J.; Xu, J.; Chen, D.C.; Wang, Z.; Li, Q.Q. Overall review of peak shaving for coal-fired power units in China. *Renew. Sustain. Energy Rev.* **2016**, *54*, 723–731. [CrossRef]
12. Simopoulos, D.N.; Kavatza, S.D.; Vournas, C.D. An enhanced peak shaving method for short term hydrothermal scheduling. *Energy Convers. Manag.* **2007**, *48*, 3018–3024. [CrossRef]
13. Xie, M.F.; Zhou, J.Z.; Li, C.L.; Lu, P. Daily Generation Scheduling of Cascade Hydro Plants Considering Peak Shaving Constraints. *J. Water Resour. Plan. Manag.* **2016**, *142*, 04015072. [CrossRef]
14. Su, C.G.; Cheng, C.T.; Wang, P.L. An MILP Model for Short-term Peak Shaving Operation of Cascaded Hydropower Plants Considering Unit Commitment. In Proceedings of the IEEE International Conference on Environment and Electrical Engineering (EEEIC)/IEEE Industrial and Commercial Power Systems Europe (I&CPS Europe), Palermo, Italy, 12–15 June 2018; pp. 1–5.
15. Wu, X.Y.; Cheng, C.T.; Shen, J.J.; Luo, B.; Liao, S.L.; Li, G. A multi-objective short term hydropower scheduling model for peak shaving. *Int. J. Elect. Power Energy Syst.* **2015**, *68*, 278–293. [CrossRef]
16. Shen, J.J.; Cheng, C.T.; Zhang, J.; Lu, J.Y. Peak Operation of Cascaded Hydropower Plants Serving Multiple Provinces. *Energies* **2015**, *8*, 11295–11314. [CrossRef]

17. Su, C.G.; Cheng, C.T.; Wang, P.L.; Shen, J.J. Optimization Model for the Short-Term Operation of Hydropower Plants Transmitting Power to Multiple Power Grids via HVDC Transmission Lines. *IEEE Access* **2019**, *7*, 139236–139248. [CrossRef]

18. Rao, A.R.; Srinivas, V.V. Regionalization of watersheds by fuzzy cluster analysis. *J. Hydrol.* **2006**, *318*, 57–79. [CrossRef]

19. Goyal, M.; Gupta, V. Identification of Homogeneous Rainfall Regimes in Northeast Region of India using Fuzzy Cluster Analysis. *Water Resour. Manag.* **2014**, *28*, 4491–4511. [CrossRef]

20. Wang, Y.T.; Chen, L.H. Multi-view fuzzy clustering with minimax optimization for effective clustering of data from multiple sources. *Expert Syst. Appl.* **2017**, *72*, 457–466. [CrossRef]

21. Yan, M.H.; Yao, X.P.; Wang, L.; Jiang, L.X.; Zhang, J.F. An analysis of the applicability of fuzzy clustering in establishing an index for the evaluation of meteorological service satisfaction. *J. Trop. Meteorol.* **2020**, *26*, 103–110.

22. Bou-Fakhreddine, B.; Abou-Chakra, S.; Mougharbel, I.; Faye, A.; Pollet, Y. Short-term hydro generation scheduling of cascade plants operating on Litani River project—Lebanon. In Proceedings of the 3rd International Conference on Renewable Energies for Developing Countries (REDEC), Beirut, Lebanon, 13–15 July 2016; pp. 1–6.

23. Nabavi-Pelesaraei, A.; Bayat, R.; Hosseinzadeh-Bandbafha, H.; Afrasyabi, H.; Chau, K.W. Modeling of energy consumption and environmental life cycle assessment for incineration and landfill systems of municipal solid waste management—A case study in Tehran Metropolis of Iran. *J. Clean. Prod.* **2017**, *148*, 427–440. [CrossRef]

24. Siu, T.K.; Nash, G.A.; Shawwash, Z.K. A practical hydro, dynamic unit commitment and loading model. *IEEE Trans. Power Syst.* **2001**, *16*, 301–306. [CrossRef]

25. Zhao, T.T.G.; Zhao, J.S.; Yang, D.W. Improved Dynamic Programming for Hydropower Reservoir Operation. *J. Water Resour. Plan. Manag.* **2014**, *140*, 365–374. [CrossRef]

26. Feng, Z.K.; Niu, W.J.; Cheng, C.T.; Wu, X.Y. Optimization of hydropower system operation by uniform dynamic programming for dimensionality reduction. *Energy* **2017**, *134*, 718–730. [CrossRef]

27. Hota, P.K.; Barisal, A.K.; Chakrabarti, R. An improved PSO technique for short-term optimal hydrothermal scheduling. *Electr. Power Syst. Res.* **2009**, *79*, 1047–1053. [CrossRef]

28. Yuan, Y.B.; Yuan, X.H. An improved PSO approach to short-term economic dispatch of cascaded hydropower plants. *Kybernetes* **2010**, *39*, 1359–1365. [CrossRef]

29. Bi, W.; Dandy, G.C.; Maier, H.R. Improved genetic algorithm optimization of water distribution system design by incorporating domain knowledge. *Environ. Model Softw.* **2015**, *69*, 370–381. [CrossRef]

30. Yazdi, J.; Moridi, A. Multi-Objective Differential Evolution for Design of Cascade Hydropower Reservoir Systems. *Water Resour. Manag.* **2018**, *32*, 4779–4791. [CrossRef]

31. Madani, K.; Lund, J.R. A Monte-Carlo game theoretic approach for Multi-Criteria Decision Making under uncertainty. *Adv. Water Resour.* **2011**, *34*, 607–616. [CrossRef]

32. Ji, C.M.; Jiang, Z.Q.; Sun, P.; Zhang, Y.K.; Wang, L. Research and application of multidimensional dynamic programming in cascade reservoirs based on multilayer nested structure. *J. Water Resour. Plan. Manag.* **2015**, *141*, 04014090. [CrossRef]

33. Mandal, K.K.; Chakraborty, N. Parameter study of differential evolution based optimal scheduling of hydrothermal systems. *J. Hydro-Environ. Res.* **2013**, *7*, 72–80. [CrossRef]

34. Li, X.; Li, T.J.; Wei, J.H.; Wang, G.Q.; Yeh, W.W.G. Hydro Unit Commitment via Mixed Integer Linear Programming: A Case Study of the Three Gorges Project, China. *IEEE Trans. Power Syst.* **2014**, *29*, 1232–1241. [CrossRef]

35. Conejo, A.J.; Arroyo, J.M.; Contreras, J.; Villamor, F.A. Self-scheduling of a hydro producer in a pool-based electricity market. *IEEE Trans. Power Syst.* **2002**, *17*, 1265–1271. [CrossRef]

36. Rodríguez, J.A.; Anjos, M.F.; Côté, P.; Desaulniers, G. MILP Formulations for Generator Maintenance Scheduling in Hydropower Systems. *IEEE Trans. Power Syst.* **2018**, *33*, 6171–6180. [CrossRef]

37. Babayev, D.A. Piece-wise linear approximation of functions of two variables. *J. Heuristics* **1997**, *2*, 313. [CrossRef]

38. Kang, C.X.; Chen, C.; Wang, J.W. An efficient linearization method for long-term operation of cascaded hydropower reservoirs. *Water Resour. Manag.* **2018**, *32*, 3391–3404. [CrossRef]

39. Shen, J.J.; Cheng, C.T.; Cheng, X.; Lund, J.R. Coordinated operations of large-scale UHVDC hydropower and conventional hydro energies about regional power grid. *Energy* **2016**, *95*, 433–446. [CrossRef]

40. Cai, Q.; Le, L. Renewable Electricity Pricing Mechanism Formation Mechanism Model Prediction. In Proceedings of the 3rd International Conference on Applied Engineering, Wuhan, China, 22–25 April 2016; pp. 1243–1248.

41. Kang, C.X.; Guo, M.; Wang, J.W. Short-Term Hydrothermal Scheduling Using a Two-Stage Linear Programming with Special Ordered Sets Method. *Water Resour. Manag.* **2017**, *31*, 3329–3341. [CrossRef]